Journal of the European Ceramic Society 23 (2003) 637–646

www.elsevier.com/locate/jeurceramsoc

Stress relaxation in the extrusion of pastes

S. Chou, K. Sydow, P.J. Martin, J. Bridgwater, D.I. Wilson*

Department of Chemical Engineering, New Museums Site, Pembroke Street, Cambridge CB2 3RA, UK

Received 5 January 2002; received in revised form 10 April 2002; accepted 28 April 2002

Abstract

Stress relaxation following the sudden halt of ram extrusion was studied over a range of die geometries and extrusion speeds using an alumina paste (solids volume fraction, $\phi = 0.62$) and a talc paste ($\phi = 0.51$). Distinctly different relaxation characteristics were observed. The alumina paste exhibited a rapid decay to give residual stresses in reasonable agreement with a model based on the pseudo-plastic rheological characterisation described by Benbow and Bridgwater. Although similar forces were required to extrude the talc paste, it showed a heavily damped decay with two time constants. The talc paste also continued to extrude slowly after the ram had stopped. This behavior was attributed to differences in ϕ and the contribution, and dissipation, of liquid pore pressures. However, increasing the solids volume fraction in the talc paste led to behaviour similar to that exhibited by the alumina paste.

Keywords: Al_2O_3; Extrusion; Forming; Paste; Relaxation; Talc; Visco-elasticity

1. Introduction

The flow behaviour of highly concentrated solid–liquid suspensions, or pastes, has received extensive coverage in the ceramics literature because of the importance of extrusion and casting manufacturing techniques. Interest in the topic from other industrial sectors, e.g. agrochemicals and detergents, has increased recently because of the need to generate products with controlled shape, high density and other attributes. Particle-particle interactions and the use of non-Newtonian liquid phases result in these materials exhibiting non-Newtonian behaviour, particularly as the solids volume fraction, ϕ, exceeds 50% and approaches the maximum packing fraction.[1] Features such as wall slip[2] and yield stress behaviour are frequently reported, rendering rheological characterisation and subsequent process modelling difficult. Most rheological measurements are made in the steady state, but paste manufacturing operations require an understanding of both steady and unsteady state behaviour in order to design process equipment, and avoid hazardous operation. With pastes, the extrapolation of steady state information to the unsteady state is complicated by (i) the uncertainty in the constutive models used, particularly as these may not agree sufficiently well with data; and (ii) the inherently inhomogeneous nature of pastes, whereby stresses may be unevenly distributed between the liquid and solid phases, which may subsequently respond to changes in stress via different mechanisms and therefore over different timescales. Even when operating in the steady state, the liquid phase may re-distribute relative to the solids phase, resulting in loss of process performance and product uniformity.[3] This inherent inhomogeneity, which is also manifest in the non-isotropic behaviour of ceramic and other 'greens' under strain (weak in tension cf. strong in compression), is likely to limit the applicability of methods developed for visco-elastic fluids to paste dynamics.

This paper describes an experimental investigation of the important case of sudden stops and starts during steady extrusion. The experiments were based around a ram extrusion configuration, as displacements and stresses could therefore be readily controlled or monitored. One aim of the work was to quantify the manner in which stresses in the material and apparatus changed after a process upset (e.g. a sudden stop to the flow). The stresses developed could lead to an operating hazard, and it is important to establish whether these would be significant. Another aim was to explore the effect of formulation on paste behaviour, achieved here by comparing an α-alumina-based ceramic paste with a

* Corresponding author. Tel.: +44-1223-334-777; fax: +44-1223-334-796.

E-mail address: ian_wilson@cheng.cam.ac.uk (D.I. Wilson).

0955-2219/02/$ - see front matter
PII: S0955-2219(02)00159-0

Nomenclature

D	diameter of die land (m)
D_0	diameter of barrel (m)
L	length of die land (m)
m	paste characterisation parameter: velocity index, die entry (m): dimensionless
n	paste characterisation parameter: velocity index, die land (m): dimensionless
P	steady flow extrusion pressure (Pa)
P_1	die entry work term in Eq. (1) (Pa)
P_2	die land work term in Eq. (1) (Pa)
P_F	residual extrusion pressure (Pa)
P_{F1}	initial residual extrusion pressure, talc paste (Pa)
P_{F2}	intermediate residual extrusion pressure, talc paste (Pa)
V	mean extrudate velocity in die land; extrudate exit velocity (m /s)
α	paste characterisation parameter: velocity dependency factor, die entry [Pa (s/m)^m]
β	paste characterisation parameter: velocity dependency factor, die land [Pa (s/m)^n]
ϕ	solids volume fraction (–)
α_0	paste characterisation parameter: yield stress factor, die entry (Pa)
τ_0	paste characterisation parameter: yield stress factor, die land (Pa)

talc-based paste of different voidage and liquid phase composition.

The rheological behaviour of the materials employed has been characterised using the approach described by Benbow and Bridgwater,[4] which is a development of that of Ovenston and Benbow,[5] for the analysis of ceramics and clays undergoing extrusion. The force required to extrude the material through with dimensions shown in Fig. 1, expresssed as an average 'extrusion pressure', P, is modelled as:

$$P = P_1 + P_2 = 2(\sigma_o + \alpha V^m)\ln[D_o/D] + 4(\tau_o + \beta V^n)\left[\frac{L}{D}\right] \quad (1)$$

where V is the velocity of the extrudate, calculated by assuming that the paste is effectively incompressible and undergoes slip in the die land. The first term, P_1, describes the work done in the die entry, and assumes that it is dominated by plastic deformation rather than interface shear. The second term, P_2, represents slip flow in the die land, ignoring any transients or entry effects. The terms in V reflect shear rate dependencies which are difficult to scale to the geometry of the system. Further discussion of the applicability of Eq. (1) can be found in Blackburn et al.[6]

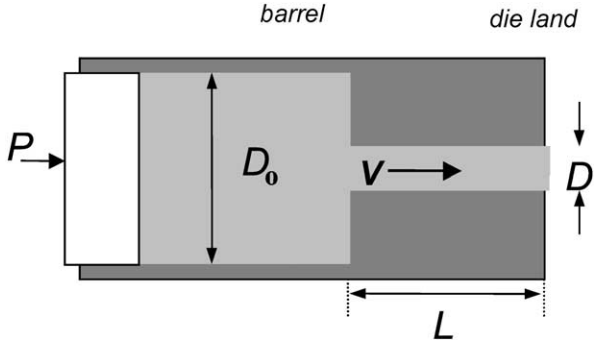

Fig. 1. Schematic of concentric cylindrical extrusion die configuration.

Inspection of Eq. (1) indicates that an initial estimate of the stresses present in an extruding system following a sudden stop in the driving auger or ram can be obtained by setting V to zero, namely

$$P_F = 2(\sigma_o)\ln[D_o/D] + 4(\tau_o)\left[\frac{L}{D}\right] \quad (2)$$

This assumes that the interactions between particles, liquid and interfaces under dynamic conditions is conserved in the static case. Exact agreement is unlikely as static and dynamic coefficients of friction are frequently reported to differ, and the slip condition in the die land is often attributed to the presence of a region of rarefied suspension or lubricating liquid film.[2] The materials used in this work were characterised using the approach described by Benbow and Bridgwater, and the residual stresses compared with those predicted by Eq. (2).

Relatively little has been reported on the phenomenon of stress decay in pastes. One study we are aware of is the work by Delalonde et al.,[7] who employed a compresso-rheometer to characterise the rheology of wet powders. This device resembled the barrel section of a capillary rheometer, and was used to assess extrusion or compressibility characteristics. They reported the stress relaxation for a micro-crystalline cellulose/water mixture, which they described as visco-elastic. The mixture composition (54.5 wt% cellulose) corresponded to $\phi = 0.35$, which is lower than usually found in materials characterised using the Benbow–Bridgwater approach.

2. Experimental

2.1. Paste preparation

Both pastes were based on commercial formulations; the alumina paste mimicked a ceramic catalyst mixture, whereas the talc paste was a placebo representing a

paste used in the manufacture of water dispersible granules. The α-alumina powders were irregularly shaped and the proportions were selected to give a solids matrix with very low permeability,[4] whereas the talc powder consisted of thin platelets. Both pastes were prepared and tested at room temperature.

The composition of the α-alumina based paste used is given in Table 1. Starch and bentonite clay were added as 'viscosity modifiers', but these insoluble components also contribute significantly to the solids volume fraction, giving a solids volume fraction, ϕ, of 0.62 and a mobile liquid phase volume fraction of 0.38. The maximum solids packing fraction of this formulation, ϕ_{max}, was estimated at 0.71 by uniaxial compaction tests to 100 MPa, giving a ratio ϕ/ϕ_{max} of 0.87. The starch particles were approximately spherical, of comparable dimension to the smallest alumina powder, and so also affect the permeability of the solids matrix. The powders were dry mixed for 10 min in a Hobart AE200 planetary mixer at the lowest speed setting, before water was added in stages and the wet mass mixed for a further 10 min. The resultant crumb was then passed twice through a high shear mixer (pugging) to break down agglomerates and distribute liquid evenly. The paste was stored in sealed bags before use in order to avoid evaporation.

The talc paste composition is given in Table 2. This paste featured a higher liquid phase volume fraction and a more complex liquid phase. The maximum solids packing fraction was estimated by compaction testing to be 0.75, giving a ϕ/ϕ_{max} ratio of 0.68. It should be noted that the differences in particle shape, size distributions (and therefore packing characteristics) make it very difficult to compare 'pastes' with such different component particles. The Morwet components are anionic surfactants and were present in solution above their critical micelle concentration, giving an apparent viscosity of 13.4 cP (apparent shear rates of 10–40 s^{-1}). The paste was prepared in a similar manner to the ceramic paste.

2.2. Extrusion experiments

Extrusion experiments were performed using a 100 kN SA100 Twin Screw Loading Frame (Dartec Ltd, Stourbridge, UK) configured to operate as a ram extruder. Paste was loaded into a 25 mm i.d. cylindrical barrel and extruded by a ram connected to the moving crosshead of the strain frame. Paste was extruded downwards through square-ended, concentric capillary dies located directly beneath the barrel in a mount. After loading, the paste was pre-compacted to a fixed average load (0.5 kN, corresponding to a mean normal stress of 1 MPa for the alumina paste: 2 kN for the talc paste). Normal stresses were recorded by the load cell in the cross-head or by pressure transducers located at the die face; the latter did not include any contributions due to interface friction at the barrel wall, which changed over an extrusion experiment as the height of the paste billet decreased. Experiments were performed in triplicate and the variation between runs was found to be much greater than any error in the displacement or force transducers.

The rheological properties of each paste undergoing extrusion was determined by the Benbow–Bridgwater approach, described previously.[4] A series of extrusion experiments through concentric, square entry dies with $D = 3$ mm and $L/D = 2$, 4, 8, 12 and 16 were performed over a range of ram velocities and the steady state data fitted to Eq. (1). The parameters obtained are given in Table 3. The Table also shows the extrusion pressure

Table 1
Formulation of α-alumina ceramic paste

Component	Supplier	Mean particle size/μm	Mass fraction (wet basis)	Volume fraction
α-Alumina F1500	Universal Abrasives Ltd, Stafford, UK	2.0	0.263	0.17
α-Alumina F600		9.3	0.263	0.17
α-Alumina F280		36.5	0.263	0.17
Native starch	Merck Ltd, Poole, UK	<3	0.030	0.05
Bentonite	Steetley Bentonite and Absorbents, Nottingham, UK	<3	0.030	0.06
Water	Reverse osmosis	–	0.150	0.38

Table 2
Formulation of talc paste

Component	Supplier	Mean particle size (/μm)	Mass fraction w.b.	Volume fraction
Talc AT Extra	Norwegian Talc, UK		0.708	0.508
Morwet EFW	Witco Corp, Houston, TX, USA	–	0.083	0.492
Morwet D-425		–	0.042	
Water	Reverse osmosis	–	0.150	

Table 3
Paste characterisation parameters

Parameter	Alumina paste[8]	Talc paste
σ_o	0.33 MPa	0.08 MPa
α	0.77 MPa s m^{-1}	1.02 MPa $s^{0.16}$ $m^{-0.16}$
m	1.0	0.16
τ_0	0.024 MPa	0.00 MPa
β	0.12 MPa s^1 m^{-1}	0.224 MPa $s^{0.26}$ $m^{-0.26}$
n	1.0	0.26
P_{est} (1 mm/s)[a]	2.08 MPa	4.91 MPa
P_{est} (2.5 mm/s)[a]	2.62 MPa	5.85 MPa
P_F[a]	1.72 MPa	0.35 MPa

[a] Extrusion pressure estimated using Eq. (1) at given ram velocity, die: $D_0 = 25$ mm, $D = 3$ mm, $L = 12$ mm.

estimated for steady extrusion through a die with $L/D = 12/3$ mm/mm at ram velocities of 1 and 2.5 mm/s, being the speeds used in the relaxation tests. The talc paste required larger stresses for a given extrusion rate, even though it had a smaller value of ϕ. Comparison of the P and P_F terms, however, indicated that the strain rate dependent contribution was more significant for the talc paste. It should be noted that a priori prediction of magnitudes of the Benbow–Bridgwater parameters is currently not available, particularly for non-spherical particulates. The same materials of construction, principally 304 stainless steel, were used in the characterisation and relaxation experiments.

Relaxation experiments were performed in the ram extrusion apparatus operating in controlled strain mode. The ram was programmed to move at constant velocity over a set displacement (±4 μm), followed by a relaxation period at zero velocity, and the sequence repeated two or three times. The whole procedure was repeated three times and data were collected every 500 ms on a dedicated PC. Fig. 2 shows the load cell data collected during repeated runs with the ceramic paste at a ram velocity of 1 mm/s. Fig. 2 illustrates the degree of reproducibility observed in these tests. After an initial transient, where flow patterns were established and material entered the die land, the extrusion pressure reached a reasonably uniform value. The extrusion

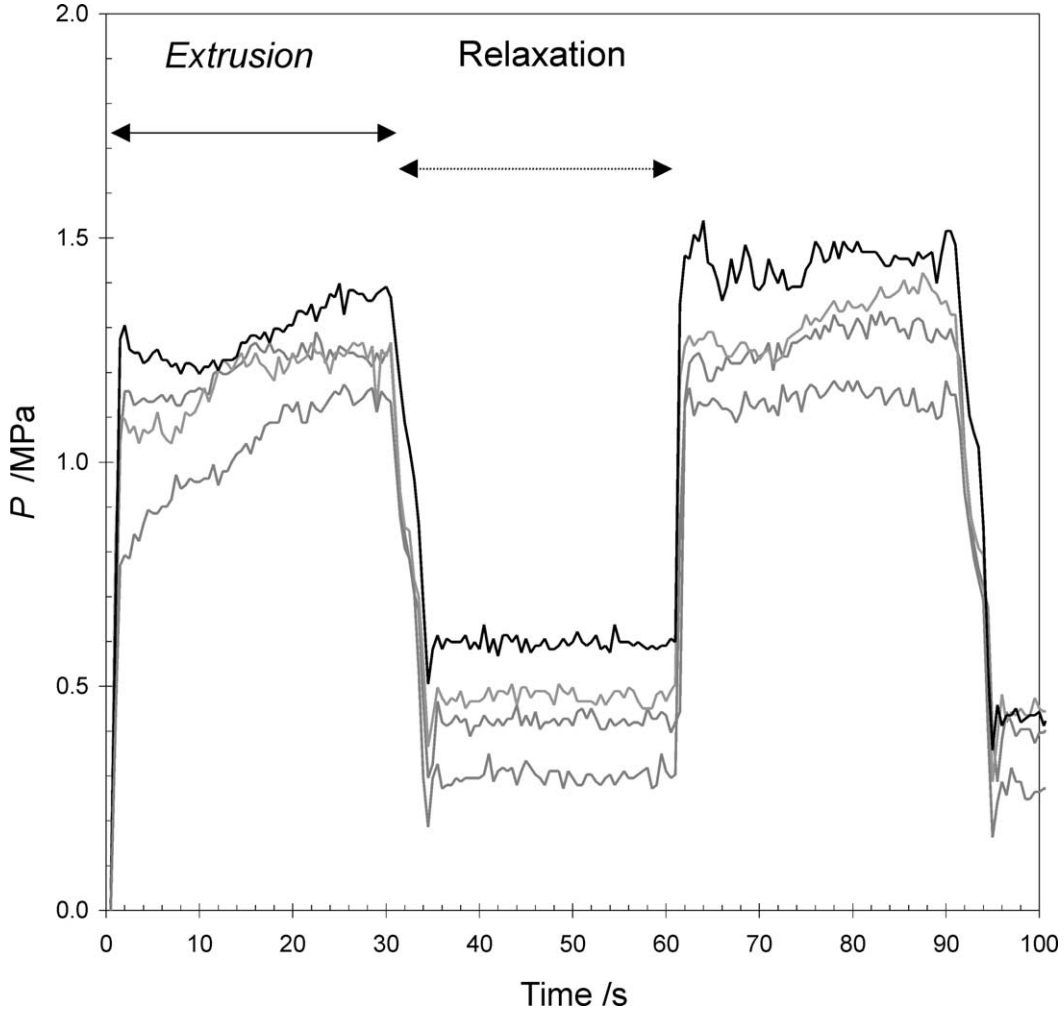

Fig. 2. Extrusion pressure – time profiles for ceramic paste. Ram velocity = 1 mm/s; $L/D = 12/3$ mm/mm.

pressure measured by the load cell decreased noticeably with displacement in talc paste experiments, as barrel wall friction was significant. The stress decay following the halting of the ram was analysed in terms of the stress reached in the static period, and the time taken to reach this stress level.

3. Results and discussion

3.1. Ceramic paste

Relaxation experiments were performed with dies of 3 mm i.d. and lengths of 0, 1, 3, 6, 12, 24, 36 and 48 mm.

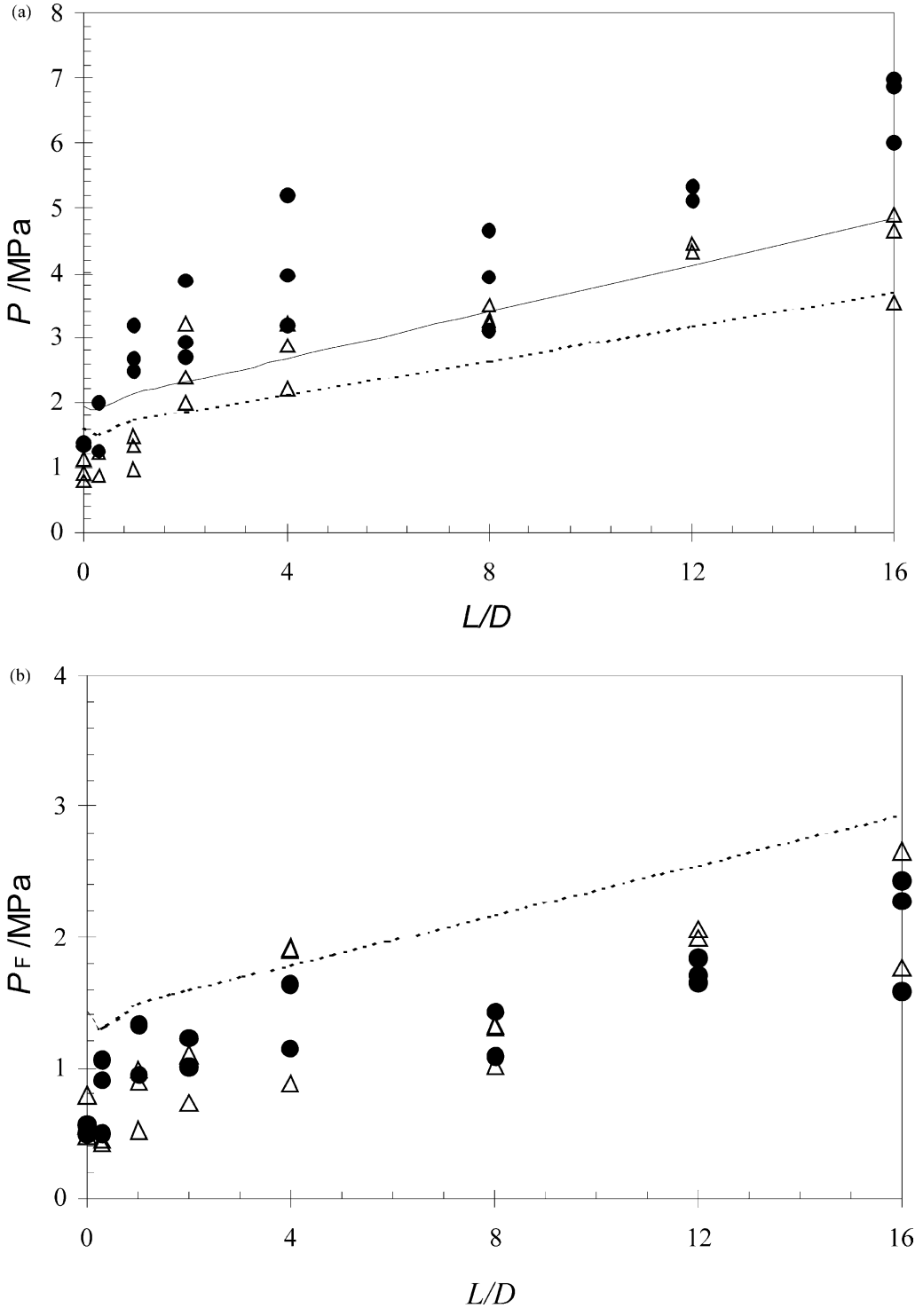

Fig. 3. Variation of (a) extrusion pressure P and (b) residual stress P_F with L/D for ceramic paste. $D_0 = 25$ mm; $D = 3$ mm. Symbols—experimental data; lines—model. Circles and solid line—ram velocity = 2.5 mm/s; triangles and dashed line—ram velocity = 1 mm/s.

Narrower dies were not used owing to the abrasive nature of the alumina. Fig. 2 shows that the stresses in this material relaxed to a finite value rapidly on cessation of ram motion, and remained reasonably constant thereafter. Experiments were also performed with relaxation periods of up to one hour between consecutive extrusions, and the P_F reading, as defined by Eq. (2), did not vary significantly. The time taken to reach the final static stress was around 5.5 s over all speeds tested. Detailed examination indicated that the stress decayed in an almost linear manner over time, and did not decrease exponentially, which one may expect from a viscous response. The length of the initial decay (5.5 s) was found to be a characteristic of the machine's displacement control; this period could be shortened by stopping the experiment completely, but this approach would not allow cyclic testing as performed here. Experiments using cyclic and interrupted testing indicated that the value of the residual stress reached was not affected by the cessation mode.

The extrusion pressures recorded during the dynamic and static periods are plotted in Fig. 3(a) and (b) respectively. The dynamic data show an approximately linear increase in P with L/D, as given by Eq. (1), with noticeable scatter in the data. This linear behaviour did not extrapolate to small L/D values, where noticeable extrudate fracture was observed, indicating that steady flow was not established. This is consistent with previous work on extrudate fracture in these materials.[9] Also shown on Fig. 3(a) are the extrusion pressures estimated for both extrusion speeds using Eq. (1) and the parameters in Table 3. The experimental values for a ram speed of 2.5 mm/s are consistently larger than the model prediction, but show the same trends. Fig. 3(b) shows that the residual stresses for both ram velocities were effectively identical, and increased linearly with L/D. The P_F values given by Eq. (2) were of the same magnitude and exhibited a very similar trend in L/D. This result suggests that the interactions involved in the τ_o term—possibly particle-wall contacts—are common to both dynamic and static cases. The main source of discrepancy between the P_F values is the deformation term (i.e. $L/D=0$), where the model overpredicted this contribution. This is likely to be due to the model including dilation work in its dynamically-based parameters, whereas dilation is not important in a static system. Measurements of extrudate and compact density indicated that dilation (or volume changes) did occur in these materials, as the extrudates were found to be consistently less dense than the compact in the barrel.

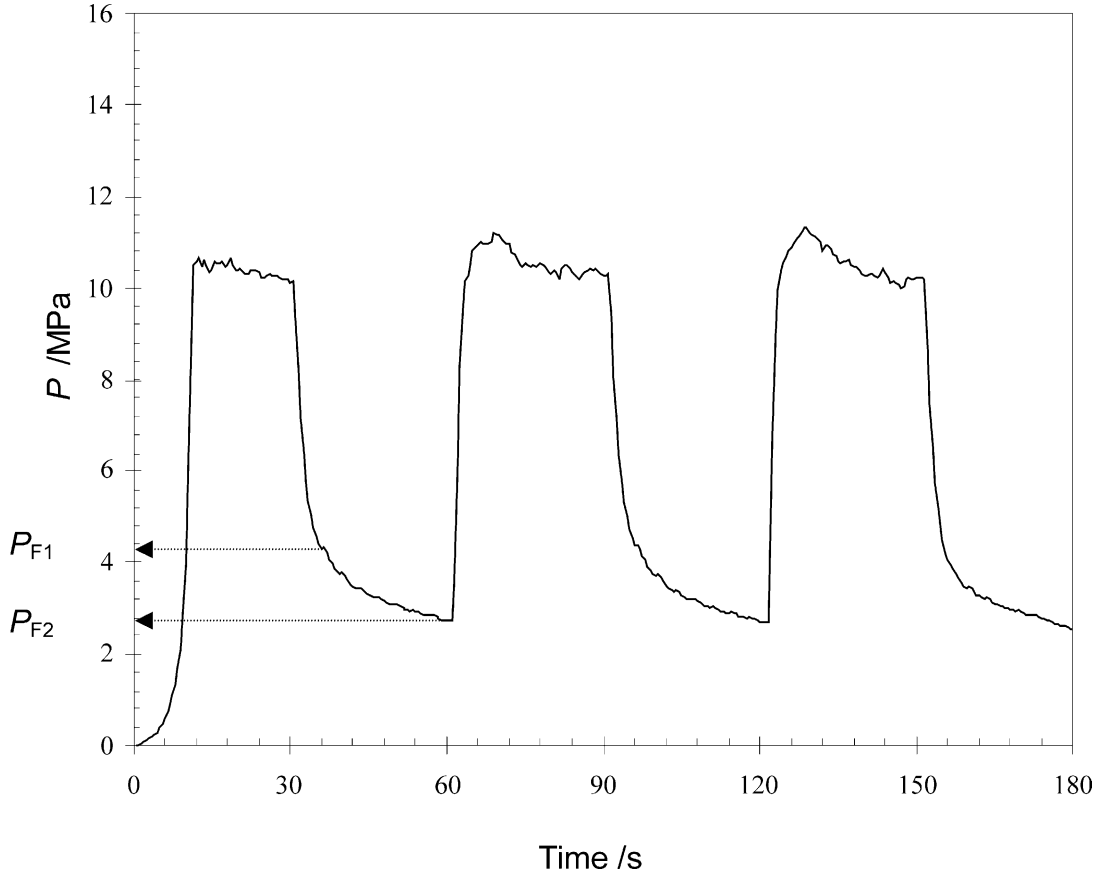

Fig. 4. Extrusion pressure – time profiles for talc paste. Ram velocity = 2.5 mm/s; $L/D = 36/3$ mm/mm.

3.2. Talc paste

Fig. 4 shows a stress relaxation profile from an experiment using the talc paste. The stress relaxation profiles all differed noticeably from the ceramic paste (Fig. 2), in that the stress decreased rapidly initially over a similar period to that observed in the alumina paste, and thereafter decayed slowly. Extended relaxation tests such as that shown in Fig. 5 indicated that the stress took approximately one hour to reach a steady residual level. The oscillations evident in Fig. 5 between 100 and 250 s were caused by the strain frame controller correcting for drift in the ram position caused by machine compliance. The logarithmic plot in Fig. 5(b) shows that the decay could not be characterised by a simple exponential decay, as two pseudo-linear regions are evident;

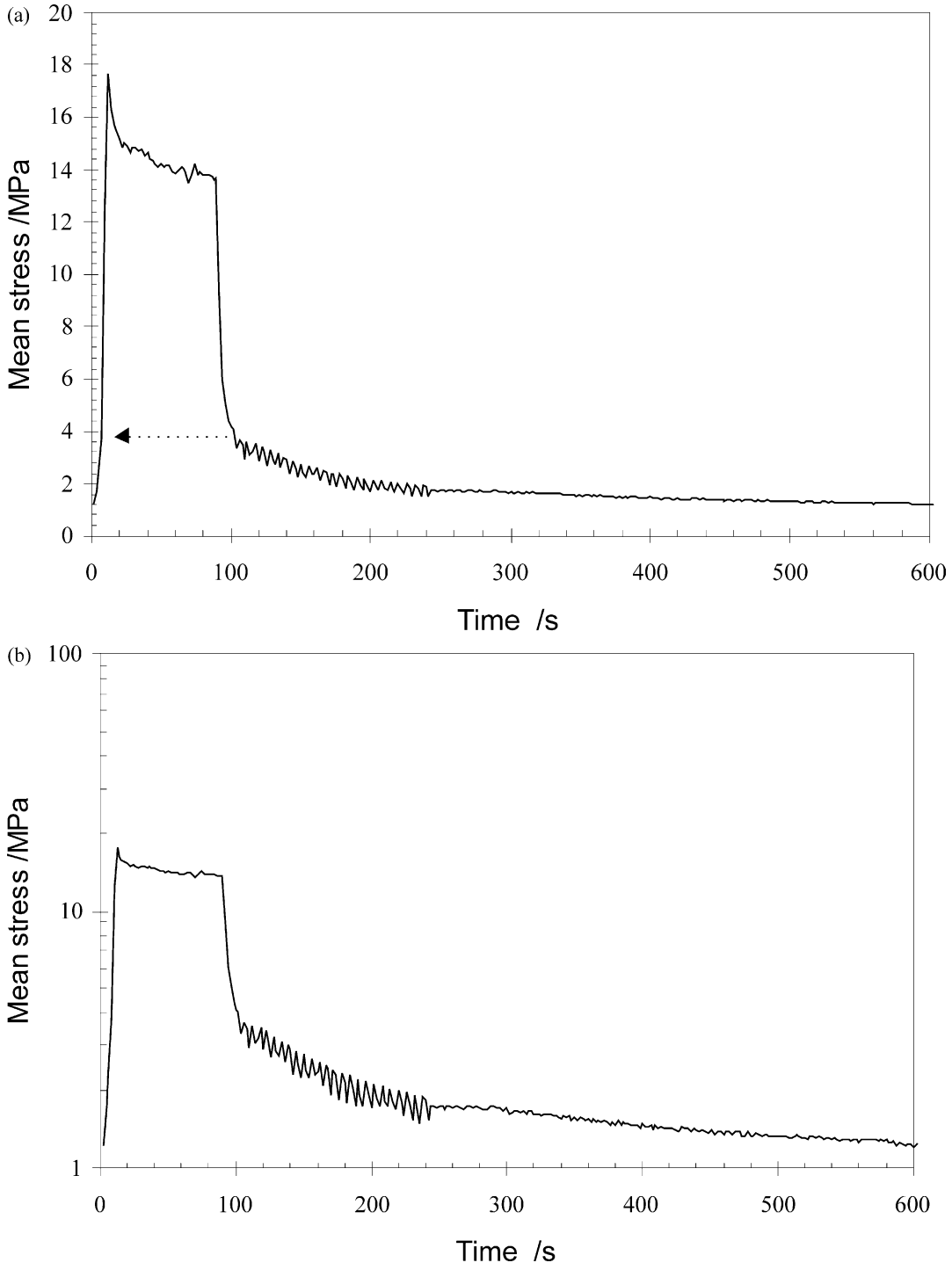

Fig. 5. Extended stress relaxation profile for talc paste: (a) linear scale; (b) log scale : $L = 48$ mm; $D = 3$ mm, ram velocity = 1 mm/s.

one from 100 to 240 s, the other when time exceeded 240 s. Moreover, material continued to extrude slowly through the die for up to 30 min after halting the ram; it should be noted that the paste did not extrude under the action of gravity alone.

The decay in residual pressure required a criterion for determining P_F. Two values were selected, as shown on Fig. 4. The first, labelled P_{F1}, was taken at the end of the initial, rapid decrease, 5–6 s after the ram was halted, corresponding to the P_F criterion for the alumina paste. The second, labelled P_{F2}, was taken at the end of the relaxation period, 30 s after the ram was halted. Both values proved to be significantly greater than P_F predicted by Eq. (2) using the parameters in Table 3. Furthermore, both the P_{F1} and P_{F2} values showed an increase with L/D, whereas Eq. (2) predicts no variation of this type since τ_o for the talc paste was found to be zero.

The decay characteristics were thus inspected further. The plot of initial reduced stress, P_{F1}, against the steady state extrusion pressure, P, in Fig. 6 shows a proportionality common to all die sizes and extrusion speeds tested, indicating that the response is determined by the material alone. Fig. 6 also shows the predicted P_F values to bear little relationship to the data. The talc response could be classed as visco-elastic, whereas the alumina paste response was almost elastic by comparison. The plot of P_{F1} against P_{F2}, recorded ~25 s later, in Fig. 7 shows that the decay characteristics were common to all die sizes and stresses, supporting the visco-elastic classification. These data correspond to a first order decay constant of 58 s.

3.3. Discussion

The two pastes displayed very different stress relaxation characteristics and suggest that different relaxation mechanisms were involved. The alumina paste, with $\phi = 0.62$, exhibited an elasto-plastic response. A high solids volume fraction will give rise to extensive networks of particle–particle contacts and thus a chiefly elastic response, possibly augmented by creep. The talc paste featured a higher liquid volume fraction (and ϕ/ϕ_{max}) and one can hypothesise that the strongly viscous response is related to the dissipation of pore pressures developed in the paste during extrusion, either by expansion or liquid phase re-distribution. The latter would be directly affected by changes in the liquid phase

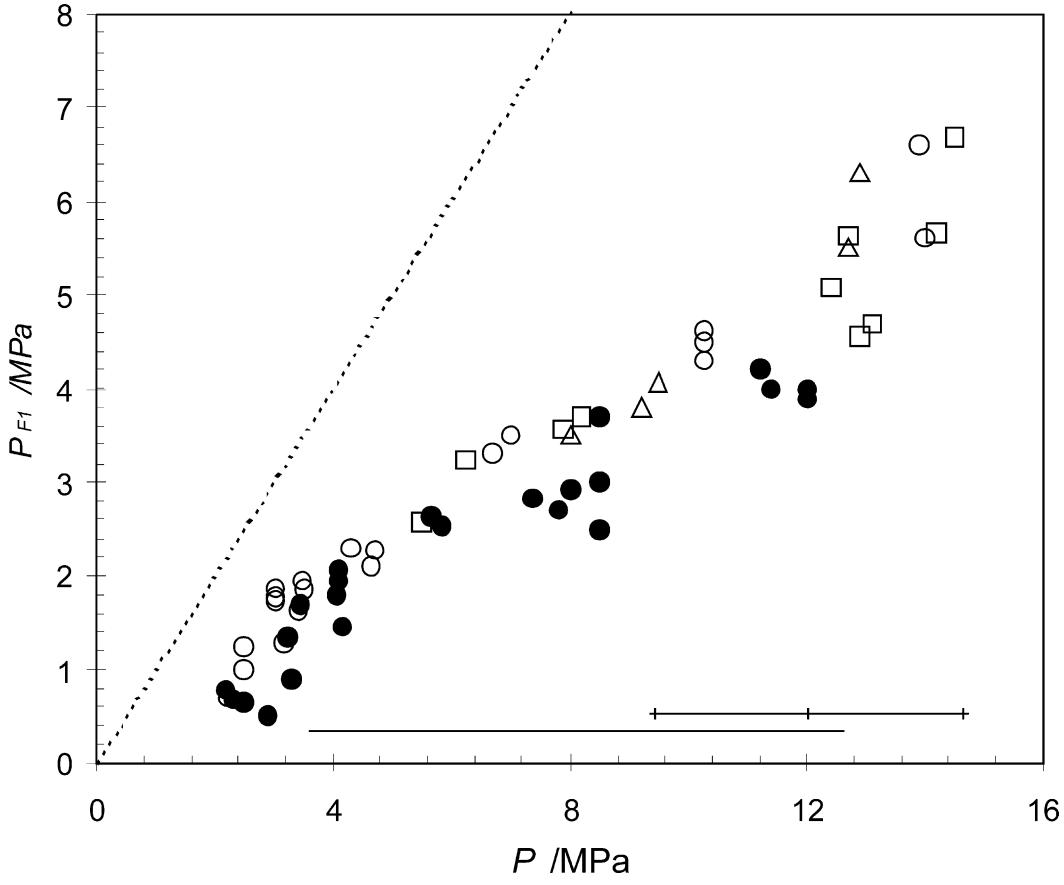

Fig. 6. Plot of initial reduced stress, P_{F1}, against steady state extrusion pressure P. Dashed line—line of equality; solid line—P_F given by Eq. (2) with talc paste parameters from Table 3 for $D = 3$ mm; crossed solid line—P_F given by Eq. (2) for $D = 1$ mm. Symbols: solid circles—$D = 3$ mm, ram speed 2.5 mm/s; open circles, $D = 3$ mm, 1 mm/s; squares—$D = 2$ mm, 1 mm/s; triangles—$D = 1$ mm, 1 mm/s.

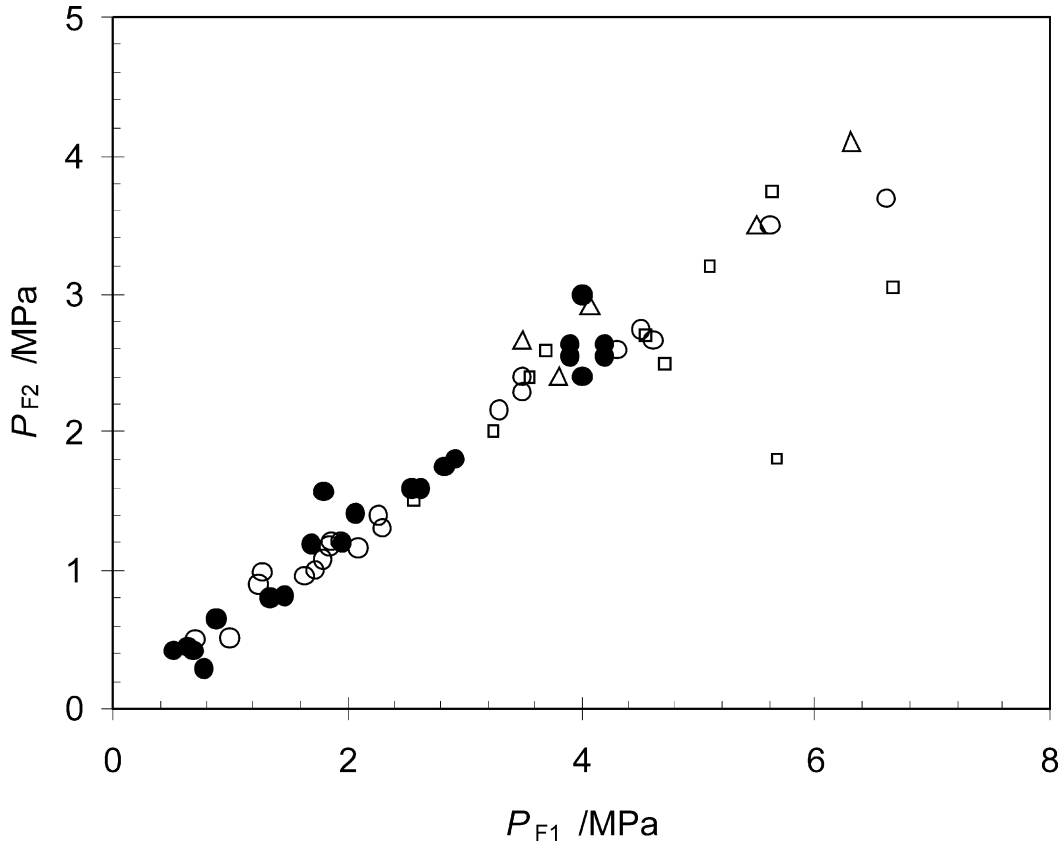

Fig. 7. Stress decay characteristic: plot of P_{F2} against P_{F1}. Symbols: solid circles—$D=3$ mm, ram speed 2.5 mm/s; open circles, $D=3$ mm, 1 mm/s; squares—$D=2$ mm, 1 mm/s; triangles—$D=1$ mm, 1 mm/s.

viscosity or solids packing characteristics, and deserves further attention. The latter is more difficult to manipulate (and measure), as the permeability of the solids matrix is determined by the particle size, volume fraction and imposed stress.

The effects of solids volume fraction in the talc paste are evident in Fig. 8, which shows extrusion and decay profiles for talc pastes with ϕ values of 0.51 and 0.55 under similar process conditions. The stresses required to extrude the talc pastes increase markedly with solids volume fraction. The maximum solids fraction at which the plate-like talc pastes with this liquid phase composition could be extruded was approximately 0.6, i.e. less than that of the ceramic paste, indicating that the particle shape is an important formulation factor. The Figure shows an initial pseudo-elastic drop in residual pressure for both pastes, to different P_{F1}/P values, and a slower stress decay in the paste with higher solids content. Similar results were observed under other operating conditions and solids fractions (up to $\phi=0.58$). The behaviour became more elasto-plastic with increase in ϕ, but decay was still evident in many cases and the observed P_{F2} values were all larger than those predicted by Eq. (2) using characterisation data generated separately.

The observed continuation of extrusion in the talc paste, albeit very slowly, during relaxation is consistent with a large hydrostatic stress and the low values of the yield parameters (σ_0, τ_0) obtained for this material. Several workers (e.g. Benbow and Bridgwater,[4] Rough et al.[10]) have reported a systematic increase in these

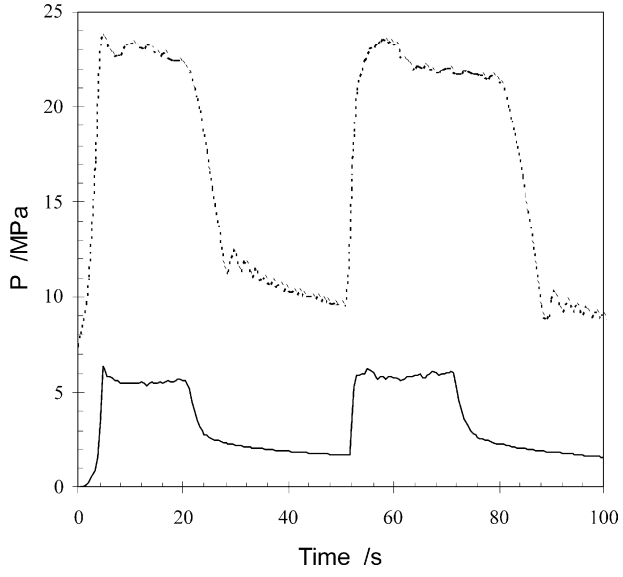

Fig. 8. Extrusion pressure—time profiles for different talc paste formulations. Solid line—$\phi=0.51$; dashed line—$\phi=0.55$. $L/D=36/3$ mm; ram velocity = 2.5 mm/s.

yield parameters with solids volume fraction, which can be attributed to increasing importance of particle interactions in flow behaviour. This work suggests that the stress relaxation response of the paste will change from a mixed reponse, possibly described as visco-elastic, to more definitely elasto-plastic with increasing solids fraction. It is noteworthy that a visco-elastic decay was important at a solids volume fraction of 0.51. Determination of the decay constants involved will be of interest for manufacturing and are likely to require experimental measurement.

4. Conclusions

The characteristics of stress decay in pastes undergoing ram extrusion was studied over a range of geometrical parameters and speeds using two different paste formulations. The higher solids volume fraction alumina paste exhibited a rapid decrease to a steady residual stress which agreed with a prediction based on the Benbow–Bridgwater model. This model tended to overpredict the residual stress, which is believed to be due to the paste characterisation parameters, which were obtained from dynamic experiments, including a contribution from dilation work. A theoretical framework for removing the dilation work contribution was not available.

Although the talc paste required similar forces to extrude it, its stress relaxation behaviour was characterised by a complex decay which did not relate to the model prediction. The stress decay behaviour with the talc paste was similar over all die sizes and extrusion speeds tested, indicating that the response is determined by the material alone. This difference in behaviour is attributed to the greater liquid volume fraction in the talc paste and dissipation of pore pressures. Talc pastes with higher solids volume fractions required more work to extrude them and showed more elastic stress relaxation behaviour.

Acknowledgements

This investigation employed resources made available under EPSRC research project GR/L 25011 on Dynamics of Pastes. The authors gratefully acknowledge an EPSRC CASE Award for PJM from Syngenta and the assistance of Zlatko Saracevic and Dr. Sarah L. Rough.

References

1. Ring, T., *Fundamentals of Ceramic Powder Processing and Synthesis*, Academic Press, 1996.
2. Khan, A. U., Briscoe, B. J. and Luckham, P. F., Evaluation of wall slip in capillary extrusion of ceramic pastes. *J. Eur. Ceram. Soc.*, 2001, **21**, 483–491.
3. Rough, S. L., Bridgwater, J. and Wilson, D. I., Effects of liquid phase migration on extrusion of microcrystalline cellulose pastes. *Intl. J. Pharm.*, 2001, **204**, 117–126.
4. Benbow, J. J. and Bridgwater, J., *Paste Flow and Extrusion*. Clarendon Press, Oxford, 1993.
5. Ovenston, A. and Benbow, J. J., Effects of die geometry on the extrusion of clay-like material. *Transactions of the British Ceramic Society*, 1968, **67**, 543–567.
6. Blackburn, S., Burbidge, A. S. and Mills. H., A critical assessment of the Benbow approach to describing the extrusion of highly concentrated suspensions and pastes. In *Proc. XIIIth International Conference on Rheology*, Cambridge, 2000.
7. Delalonde, M., Baylac, G., Bataille, B., Jacob, M. and Puech, A., The rheology of wet powders: a measuring instrument, the compresso-rheometer. *Int. J. Pharm*, 1996, **130**, 147–151.
8. Domanti, A. T. J., *Surface Fracture in Paste Extrusion*. PhD Dissertation, University of Cambridge, 1998.
9. Domanti, A. T. J. and Bridgwater, J., Surface fracture in axisymmetric paste extrusion. *Trans IChemE A*, 2000, **78**, 68–78.
10. Rough, S.L., Bridgwater, J. and Wilson, D. I., Modelling of paste extrusion subject to liquid phase redistribution. In *Proc. Chemeca 2000*, Perth, WA. IchemE, Australia, pp. 400–405.